Proceedings World Geothermal Congress 2020+1
Reykjavik, Iceland, April - October 2021

Numerical Model of Wayang Windu Geothermal System to Optimize Production Strategy

Riza G. Pasikki, Boyke Bratakusuma and Mulyadi

Riza.Pasikki@starenergy.co.id ; Boyke.Bratakusuma@starenergy.co.id ; Mulyadi.S@starenergy.co.id

Keywords: Reservoir simulation, numerical model, Wayang Windu, reservoir forecast.

ABSTRACT

A full field numerical simulation model has been developed for Wayang Windu for forecasting field performance under a range of production scenarios. The quality of the history match obtained for well pressure (steam zone and liquid) and enthalpy gave confidence that the newly developed model was a reasonable predictive tool to evaluate alternative exploitation strategies, with the main focus to evaluate the capacity of the reservoir to support additional 60 MW development by 2024. The area of the commercial reservoir, interpreted from the numerical model, has excluded the northwestern region of the developed field that was previously defined as a potential commercial reservoir extension based on the location of resistivity anomalies. Therefore, the development strategy to drill in the northwestern region was not included in the reservoir forecast. Two basic development strategies were included: (1) shallow drilling in the northern steam cap supported by several shallow wells in the central area, which represents production the strategy currently applied in the Wayang Windu field; and (2) mixed shallow and deep wells. In both development strategies, the southern Windu reservoir compartment was reserved exclusively for brine and condensate injection.

The Numerical modeling indicated that the steam cap alone could not support 227 MW generation until the end of the contract period. Maintaining a right balance between production from the steam cap and deep brine reservoirs is critical to the successful management of a liquid dominated geothermal reservoir such as Wayang Windu. Based on the model, the current production scheme of producing 95% from the steam cap reservoir and 5% from the brine reservoir has caused rapid pressure decline in the steam cap reservoir section while deep-brine reservoir pressure relatively unchanged. As a result, water level in the reservoir has inclined to the shallower depth from an initial depth of around +450 m ASL elevation. The modeled response was consistent with recent measured pressure-temperature data from deep wells. The preferred resource development strategy is a combination of shallow and deep drilling which outperforms the shallow drilling strategy because: 1) a more balanced extraction from the steam cap and brine reservoir sections promotes steam cap growth; and 2) there is less production interference due to larger well separations. The model suggests that a steady production of 227 MW could be sustained until the end of the contract period. The potential upside of the reservoir was also tested with the same drilling strategy, wherein 60 MW generation (Unit-3) is added to the existing 227 MW generation by 2024. The model confirms the opportunity for Unit-3 development if a permeability of 60 millidarcy or higher is encountered in the deep brine reservoir section during the upcoming drilling programs.

1. INTRODUCTION

Recent assessment has been conducted by the Reservoir Management Group in Star Energy to evaluate whether the Wayang Windu geothermal resource could support organic growth of adding a 60 MW power plant to the existing 227 MW power plant operation until the year 2040. This resource assessment was based on the existing integrated conceptual model of the geothermal field upon evaluations of geology, geochemistry, geophysics, downhole well and discharge well data. A large number of big-hole development wells and several slim-hole exploratory wells have been drilled in and around the field, providing data on subsurface temperatures, pressures, fluid chemistry, and subsurface geology and reservoir properties. Therefore, the location, shape and appropriate extent of the Wayang Windu geothermal system have been defined reasonably well and many key characteristics of the system have been interpreted with a reasonable degree of confidence. The proven resource covers an area of 22 km^2 (Figure 1) and is closely associated with northeasterly trending volcanic domes on the southern slope of Gunung Malabar. This most likely conceptual model has been converted into a numerical model to evaluate resource performance under different generation scenarios. The new Wayang Windu numerical model has been constructed using the TOUGH2 reservoir simulator and has been calibrated against initial (pre-exploitation) reservoir pressure and temperature. In addition, it has also been calibrated against historical production observations such as steam cap reservoir pressure, liquid reservoir pressure, discharge enthalpy and superheat evolutions during 18 years of commercial operation at 110 and 227 MW loads.

To represent better the naturally fractured nature of the Wayang Windu reservoir, the numerical model was constructed using a dual porosity approach. With this approach, the model is composed of two permeable media, one of them is the rock matrix and the other the fractures. The matrix contains most of the pore space but its permeability is much lower than the fractures. The fractures, on the other hand, contain a very small pore space but their permeability is large. The two media are connected in each modeling block through a very important link called the matrix-fracture interface. Neighboring fracture elements are connected to each other and this makes it possible for the fluid to flow throughout the reservoir.

Throughout the numerical model, rock and fluid properties were specified and the production history was simulated by imposing mass extraction and injection on specific fracture blocks where the wells were completed. Pressure was monitored and compared to actual measured pressure variations and the quality of the match was conventionally associated to the quality of the model to predict future behavior.

2. NUMERICAL MODEL VARIABLES

The variables required to characterize a geothermal fractured reservoir will be discussed and their center point value presented in this section.

2.1 Model Geometry

The grid was set to allow future investigation of reservoir performance under both the base and optimistic resource areas. Therefore, the model grid covered potential reservoir area extension to the northwest as indicated by a low resistivity anomaly from magnetotelluric (MT) data. As shown in Figure 1, the model grid extended 11.5 km in the east-west direction and 16.5 km north-to-south. There were in total thirteen layers along the vertical direction to cover a reservoir section from an elevation of 1,200 to a depth of -1,700 m SL and each layer of the model was divided into 40 by 59 blocks or 2,360 blocks with a typical size of 200 by 200 by 200 m. The reason for this coarse discretization is that the implementation of a dual porosity model creates very small fracture elements. Wells are completed in these fracture elements and typical flow rates of geothermal wells are on the order of tens of kg/s of steam. These large flow rates are not numerically compatible with too small fracture blocks as the numerical solution becomes extremely slow and numerically unstable. Using a dual porosity method with MINC (Multiple interacting continua) of 2 (from layer 1 to 4) and 4 (from layer 5 to 13), the model was partitioned to have a total of 30,680 blocks.

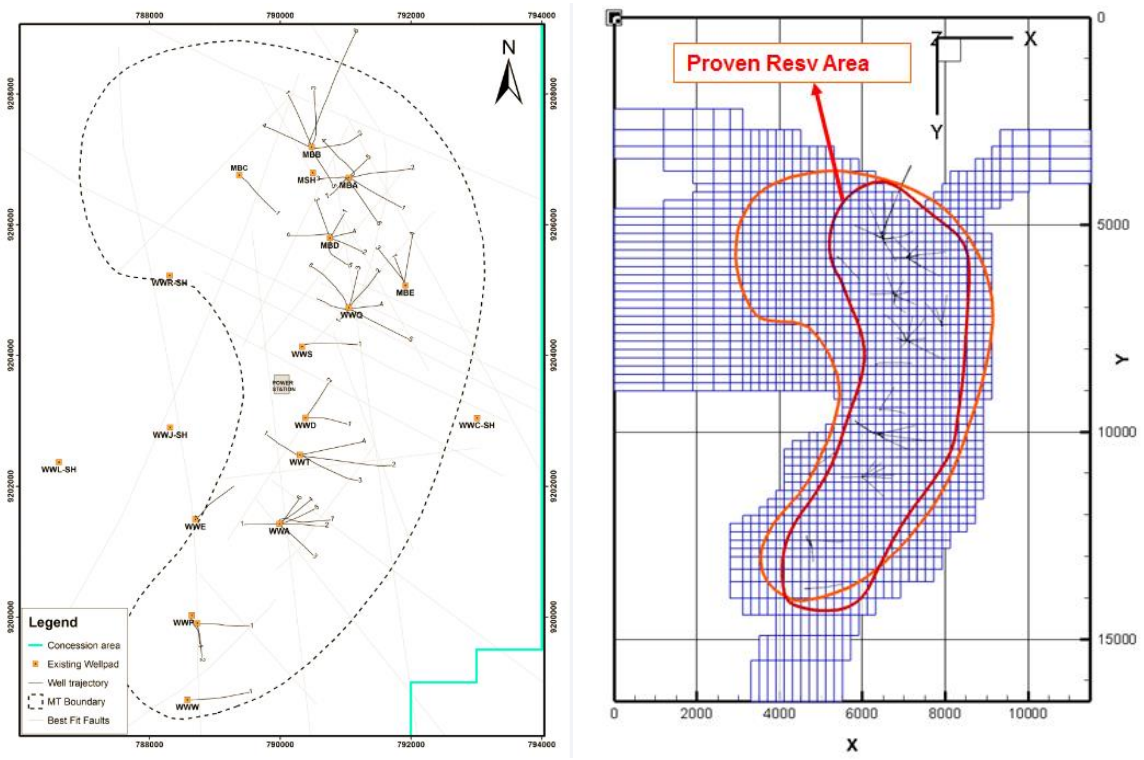

Figure 1: Map view of the Wayang Windu resource (left) and the model geometry (right).

2.2 Porosity

A non-facies approach was taken for the porosity distribution of the current Wayang Windu model. A general approach of reducing porosity with increasing depth due to increased compaction was taken with the assigned matrix porosities taking values between 3.0% and 12.5%. Unlike unfractured oil and gas reservoirs, where fluids are contained in porosity and only flow through porous space, a geothermal field's reserve is stored heat (not mass) that is uniformly distributed and flows through rock and porous space. Therefore, unlike the unfractured oil and gas reservoirs, where detailed porosity is important to show location of reserves, detailed porosity is less important for geothermal and average values are enough. In addition, the existence of fracture systems in geothermal reservoirs reduces the importance of detailed descriptions of matrix porosity distributions and allows a reliance on average values.

For naturally fractured reservoirs, it is commonly assumed that most porosity is located in the matrix while the fractures provide large-scale permeability but negligible porosity. The smaller volume elements in the model are fracture elements that consist of void volumes with no rock volume, this means that their local porosity is 100%. The bulk porosity for the fracture, however, is set at 1% (bulk porosity for the matrix is 99%). This value is a compromise that results from being small enough to represent the expected low fracture volume in a geothermal reservoir system but high enough to avoid numerical instability.

2.3 Fracture Permeability

Fracture permeability is a bulk property of the fractured medium. It is created by the combined action of fractures each one with very different local permeability values. The horizontal fracture permeability distribution in the model was initially interpreted using a property of the region close to the well called the Productivity Index (PI) using the following equations:

$$PI' = \frac{2\pi k h}{\ln\left(\frac{r_e}{r_w}\right) + S - 0.5} \tag{1}$$

$$k = \sqrt{k_x^2 + k_y^2} \tag{2}$$

PI : Permeability Index (m^3)
r_e : drainage radius (m)
r_w : well radius
S : skin
kh : fracture permeability (millidarcy – meter), where h is model block thickness
k_x : horizontal fracture permeability in X direction
k_y : horizontal fracture permeability in Y direction

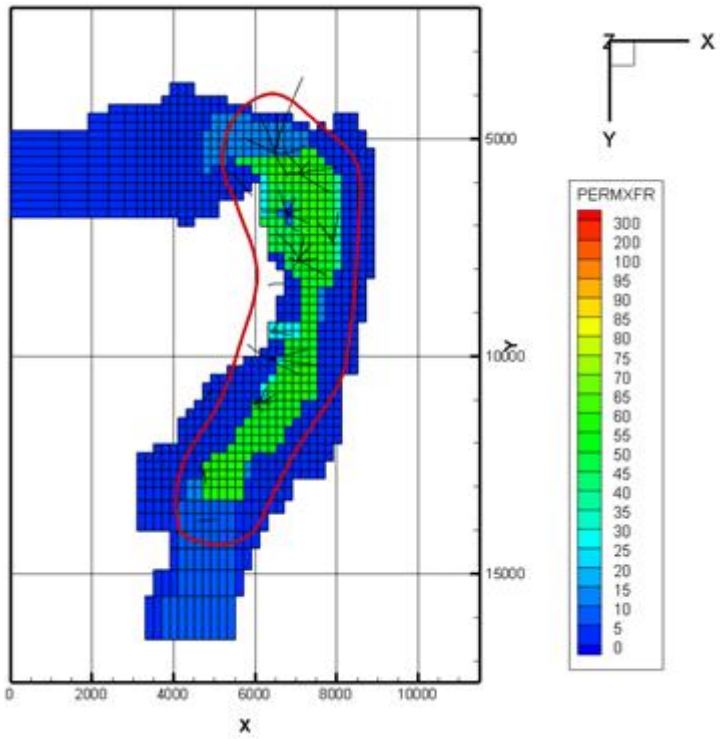

Figure 2: Fracture permeability at sea level.

PIs measured in the wells based on Pressure-Temperature-Spinner (PTS) surveys and calibrated with historical production data were used as basis for choosing the initial fracture permeability distribution in the numerical model. The assigned permeability was then calibrated to natural state and production history observations. There was no anisotropy for horizontal fracture permeability within the block model so that k_x was equal to k_y. In most blocks, the vertical fracture permeability was set at half the horizontal permeability. A map view of the central point cases for horizontal fracture permeability at sea level is shown in Figure 2. For the current reservoir model, low fracture permeability values of < 10 millidarcy were assigned to the northwestern region that was previously indicated by low-resistivity anomaly data as a potential commercial reservoir extension. A low permeability distribution to the northwest of the proven reservoir was required to obtain good matches to the pre-exploitation state and during the production period for given boundary conditions (especially with a reasonable upflow strength) as explained in later sections of this paper.

2.4 Matrix-Fracture Connection

The single-phase volumetric flow between the matrix and fractures is formulated with the following equation:

$$Q = \frac{\sigma\, k_{ma} \vartheta}{\mu} (P_{ma} - P_{fr}) \quad (3)$$

$$\sigma = \frac{C}{L^2} \quad (4)$$

Q : volumetric flow rate
σ : shape factor
k_{ma} : matrix permeability
μ : viscosity
V : the bulk volume of matrix
P_{ma} and P_{fr} : matrix and fracture pressures respectively
L : Fracture spacing
C : Shape factor constant. TOUGH2 simulator used 60

The matrix fracture connection is therefore controlled by the product of the shape factor and the matrix permeability (σk_{ma}). Matrix permeability can be measured in cores. For geothermal systems it is orders of magnitude smaller than fracture permeability. In the current model, it was assumed that the matrix permeability was isotropic. This means that values in the three main directions were the same in each simulation block. The matrix permeability currently assigned was quite homogenous: 8 microdarcy from the top of reservoir to a +400 m SL depth (steam cap reservoir section) and 5 microdarcy for all blocks located below +400 m SL (liquid reservoir section). The following Grant's curve of relative permeability functions for liquid (k_{rl}) and for steam (k_{rg}) are used:

$$k_{rl} = \hat{S}^4 \quad (5)$$

$$k_{rg} = 1 - k_{rl} \quad (6)$$

where $\hat{S} = (S_l - S_{lr})/(1 - S_{lr} - S_{gr})$ and the restrictions that $S_{lr} + S_{gr} < 1$ and $S_{lr} = 0.05$ $S_{gr} = 0$ are assigned in the fracture while $S_{lr} = 0.35$ and $S_{gr} = 0.05$ are assigned for the matrix.

The effect of changes in matrix permeability can be offset by simultaneous changes in the shape factor such that σk_{ma} remains constant. The effect of fracture spacing and matrix permeability is directly dependent on one another. The term that controls the effectiveness of the matrix-fracture connection is given by the product of matrix permeability over fracture spacing squared:

$$\sigma k_{ma} = \frac{C k_{ma}}{L^2} \quad (7)$$

The "shape factor" is nothing else than the area of interface between matrix and fracture per unit volume divided by the average distance of the fluid in the matrix to the interface. We do not know the actual geometry of the fracture system and there is no proven method to measure fracture spacing from logs. In order to define the range of possible values and based on experience, we know that the actual value is larger than the inverse of fracture density measured in image logs but smaller than the average distance between feed zones in wells. The range of fracture spacings to be used in the current model is 60 – 180 meters. The fracture spacing variable is adjusted to obtain good production history matches.

2.5 Permeability Multipliers in the X, Y, Z Directions

These three variables are used to specify the presence of a barrier or an enhanced flow channel. This is done by multiplying the area of contact between neighboring blocks by the respective parameter. A low value causes the connection of neighboring blocks to be made weaker as expected for barriers. A large value increases the interface area making it possible to create enhanced flow paths. A value of 1 will not create any change. A permeability multiplier of 0.1 was applied in the model to help create two horizontal semi-permeable barriers that help to increase the pre-exploitation temperature gradient below mean sea level (0 m SL) in liquid regions of the reservoir.

2.6 Multiple Interacting Continua (MINC)

The simulator (TOUGH2) makes it possible to discretize even further the matrix blocks in order to model in intra-matrix gradients in pressure, temperature and saturation. A parameter called MINC controls whether we discretize the matrix or not. For this case we have elected to set MINC to 2 - 4 for the Wayang Windu model.

3. NATURAL STATE MODELING AND THERMODYNAMIC INITIAL CONDITION

A geothermal reservoir is dynamical system wherein the upflow, thermal losses to surface, hot springs/fumaroles and discharge/recharge to lateral aquifers take place even before exploitation begins. Therefore, initial state (natural) simulation is a must in numerical modelling of a geothermal reservoir. This is done by placing mass/heat sources and sinks in a 3-D permeable medium and running a simulation until a steady state is achieved (>150,000 years of simulation time). Important variables to adjust during natural state modeling included:

- Location, strength of inflows (rate, enthalpy)
- Fracture permeability distribution
- Boundary conditions (aquifer, outflow, heat loss)

Measured downhole pressure and temperature from the wells from the pre-exploitation stage provided reliable constrains for calibration of the natural-state model. The variables were changed by trial and error until a good matches to initial pressures and temperatures were achieved. The results of the natural state matching were not affected by storage terms (porosity, initial water saturation) and fracture-matrix connectivity terms (fracture spacing, matrix permeability). Therefore, the later step called "production-history matching" was used to calibrate the storage and fracture-matrix connectivity terms.

3.1 Boundary Conditions

Boundary conditions at depth consist of an impermeable and constant-temperature (300°C) boundary conditions in the simulation cells located at the bottom face of the model. The upper boundary was also impermeable and had a constant temperature (20°C), and it acted as heat sink. The interface was located in the upper face of the uppermost block in each block column and the distance of the boundary condition to this interface equaled the difference in elevation between this upper face and the surface.

Natural recharge occurred at the bottom of the model in three sources located in the deepest block (Figure 3). The first one in the north called the Gambung upflow injected 29 kg/s of fluid at an enthalpy of 1402 kJ/kg. The second natural recharge called the Windu upflow located in central parts of the field near to the WWA wellpad location, injected 1432 kJ/kg of fluid at a rate of 12 kg/s. Geochemical evidence indicates that this is the most equilibrated upflow to the Wayang Windu system. Initial chloride concentration in the deep reservoir was approximately 12,000 ppm with a low gas concentration of 0.2 wt. % and the temperature in the upflow was about 310°C. The southernmost upflow is located at Gunung Windu near to the WWF and WWW wells, injecting 1432 kJ/kg fluid at a rate of 8 kg/s. This part of the field was distinguished by its brine and gas chemistry. The deep brine contained relatively low chlorides approximately 7,000 ppm and enriched with gas with concentration up to 10%. To capture geochemical evidence, a discontinuity with a high fracture permeability distribution was applied to the area near to the WWW and WWF wells. The total upflow rate was 49 kg/s.

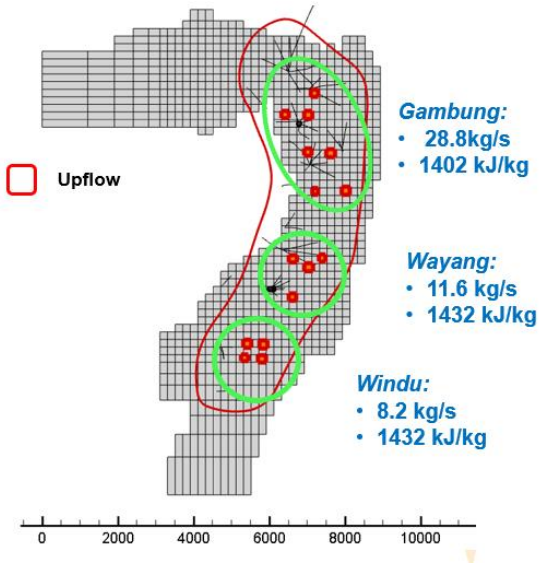

Figure 3: Upflow distributions and strengths applied in the Wayang Windu reservoir model.

The outflow was located north, close to the MBB wellpad in the uppermost block. It was simulated as a well on deliverability with a back pressure of 10 bar. Four constant pressure boundaries are also attached to the reservoir model, which act as mass sinks toward the northeast, northwest and west directions in layers 4 (elevation 500 m ASL), 6 (100 m), 7 (-100 m) and 9 (-500 m). The productivity index (PI) of the simulated wells for outflow and the pressure of the constant-pressure boundaries were adjusted to obtain good matches to pre-exploitation pressures.

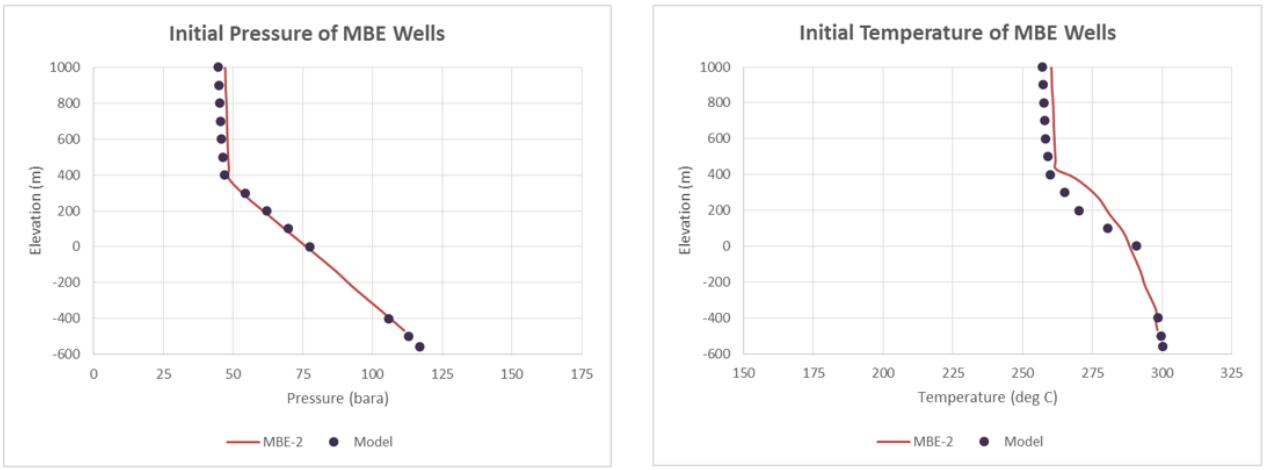

Figure 4: Initial pressure and temperature matches for the MBE-2 well.

3.2 Initial Pressure and Temperature

There are 12 wells in Wayang Windu where the pre-exploitation downhole pressure and or temperature were available: MBD-2OH, MBD-4, MBE-2, WWQ-2, WWQ-3OH, WWQ-5, WWS-1, WWD-1, WWT-1, WWA-2, WWF-1 and WWW-2. From the initial state simulation, good agreement between measured and modeled initial pressure and temperature were obtained for all those wells. Figure 4 shows the example of initial pressure and temperature matches for the MBD-2 well. In addition, the thermodynamic initial conditions below have been successfully reproduced in natural-state modeling:

- Steam to liquid contact before exploitation is located at +400 m ASL.
- At the shallow reservoir section (800 to 400 m ASL), initial temperature in the center and south was higher than that at in north reservoir part, consistent with the measured initial steam cap pressure distribution (Figure 5)
- In the liquid reservoir section in the southern part of the field, the axis of high temperature in the model was consistent with the observed high-temperature (exceeding 300ºC) trend of NE to NNE orientation and passed through the traces of the WWA and WWT wells (Figure 6).

One key insight provided by natural-state simulation was that the NW region previously defined as a potential reservoir extension based on anomaly resistivity distribution was the least likely to be part of the Wayang Windu commercial reservoir extension. With reasonable boundary conditions, low fracture permeability needs to be assigned to the NW region to obtain acceptable initial pressure and temperature matches.

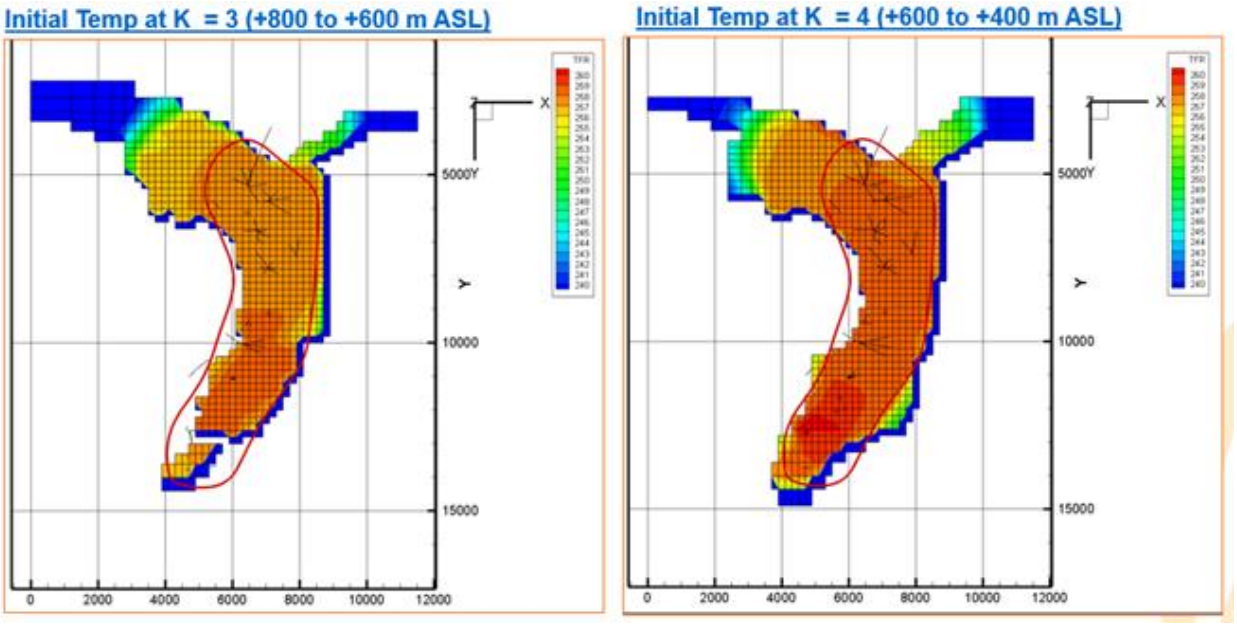

Figure 5: Initial temperature at the shallow (steam cap) reservoir section, 800 to 400 m ASL elevation.

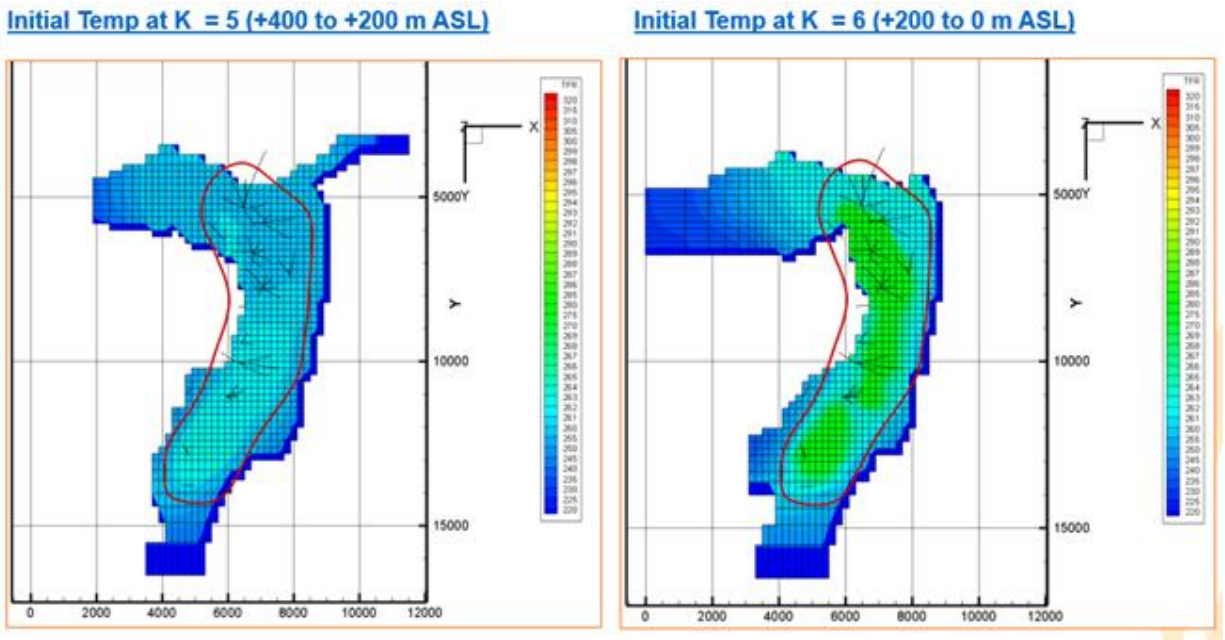

Figure 6: Initial temperature at the liquid reservoir section at an elevation from 400 to 0 m ASL.

4. PRODUCTION HISTORY MATCH

The second step of model calibration was production history matching. Stabilized pressures, temperatures and saturations resulting from the natural state simulation were used as initial conditions for the production simulation. Historical data of production rate, brine and condensate injection rate, as well as enthalpy of injected brine and condensate for the years 2000 – 2018 were imposed to run the model. History matching was then carried out using three main variables from 22 production wells: steam cap pressure, liquid pressure and discharge enthalpy measured in the individual wells. In addition, the historical evolution of superheat was also used to constrain the model.

Figure 7 shows an example plot comparing the simulated steam cap reservoir pressure profiles with the measured pressures obtained from the MBD-1 well in the north. These measured pressures were the shut-in wellhead pressures taken at wells that have steam feedzones in the central and north parts of the field. The simulated pressure was corrected to the wellhead pressure using a vapor static pressure gradient. Good matches with measurements for wells in the north (MBA, MBB, MBD and MBD) were obtained. However, historical steam cap pressure for the central wells (WWQ) for the years 2000 to 2016 could not be matched (Figure 8). Further attempts to improve the match have not been tried considering reliability of available shut in wellhead pressure data of the WWQ wells to represent the steam cap pressure. All WWQ wells were drilled to penetrate the deep liquid reservoir section. Unlike the dry steam wells in the north part of the field (MBA, MBB, MBD, MBE), the WWQ wells require a longer period of time to reach stabilized wellhead pressure under shut-in conditions, especially those that are weak wells. For the WWQ wells, steam cap pressure matching was focused on the event wherein the wells were shut-in for a long period of time such as

during field shut down for five months due to a landslide incident in 2015. Despite some discrepancies, good matches with measured data at the end of the production simulation were obtained for all of the WWQ wells, which is important to proceed with the next step of reservoir forecasting. Overall, the model can reconstruct the change of pressure decline at the steam cap reservoir due to the change of field generation from 110 to 227 MW in 2009. Simulated steam cap pressure decline rates of 0.4 bar per year before 2009 and around 1.0 bar per year after 2009 are consistent with field observations.

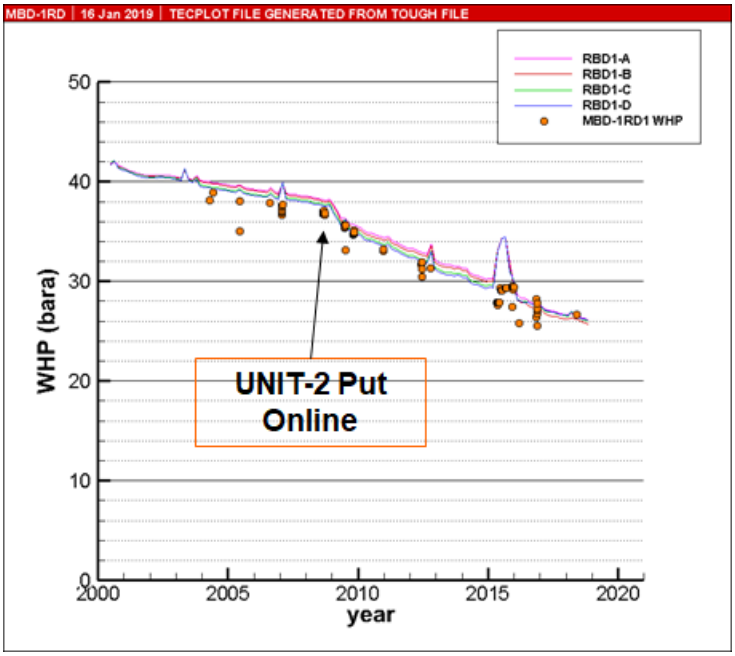

Figure 7: Steam cap pressure match for the MBD-1 well.

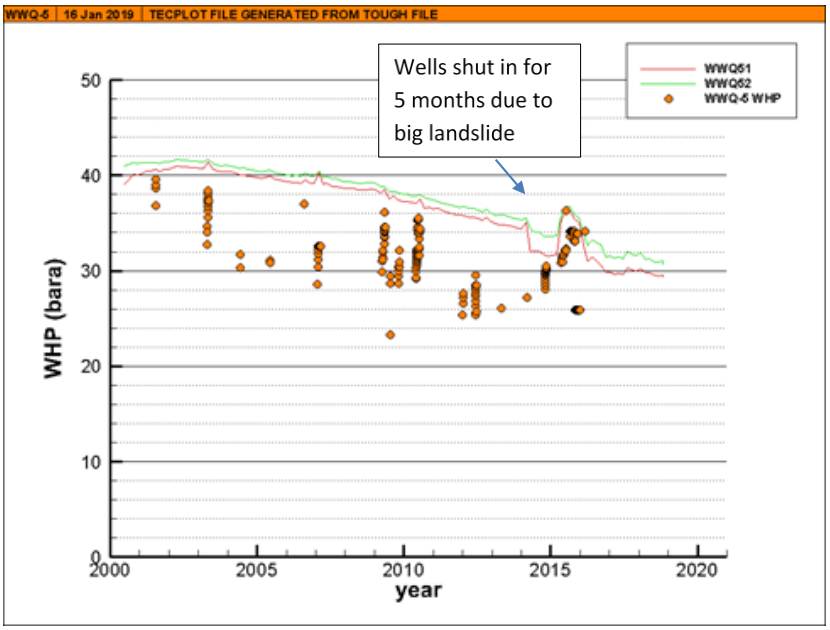

Figure 8: Steam cap pressure match for the WWQ-5 well.

Unlike the steam cap pressure trend, the amount of data to constrain the pressure-decline trend in the liquid reservoir section was relatively limited. With the absence of the continuous down-hole pressure measurement system from dedicated monitoring wells, trends of liquid reservoir pressure only derived from sporadic shut-in PT surveys. Figure 9 shows an example of reasonable matches obtained between the model and measured liquid reservoir pressure trend in the WWD-1 and WWD-2 wells. Pressure in the liquid reservoir section has been relatively stable with a maximum total pressure drop of 5 bar over 18 years of field production. This was mostly caused by the existing field production strategy in which 95% of production came from the steam cap reservoir and only 5% of steam came from the deep brine reservoir. The imbalanced extraction between the steam cap and deep brine reservoirs has not been the most optimum way to develop the Wayang Windu field since the steam cap reservoir experienced a high pressure decline rate but there has been a very low-pressure decline rate in the liquid reservoir. As a result, steam to liquid contact in the reservoir has become shallower (Figure 10). Continuing the current production strategy will cause steam feedzones to flood and eventually reduce steam production.

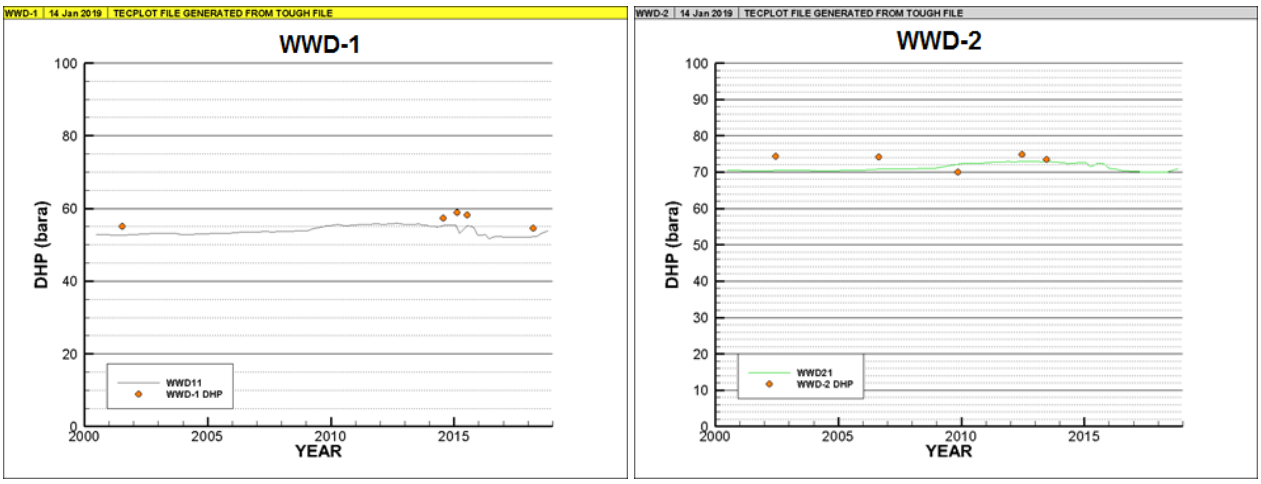

Figure 9: Liquid pressure match for wells WWD-1 and WWD-2.

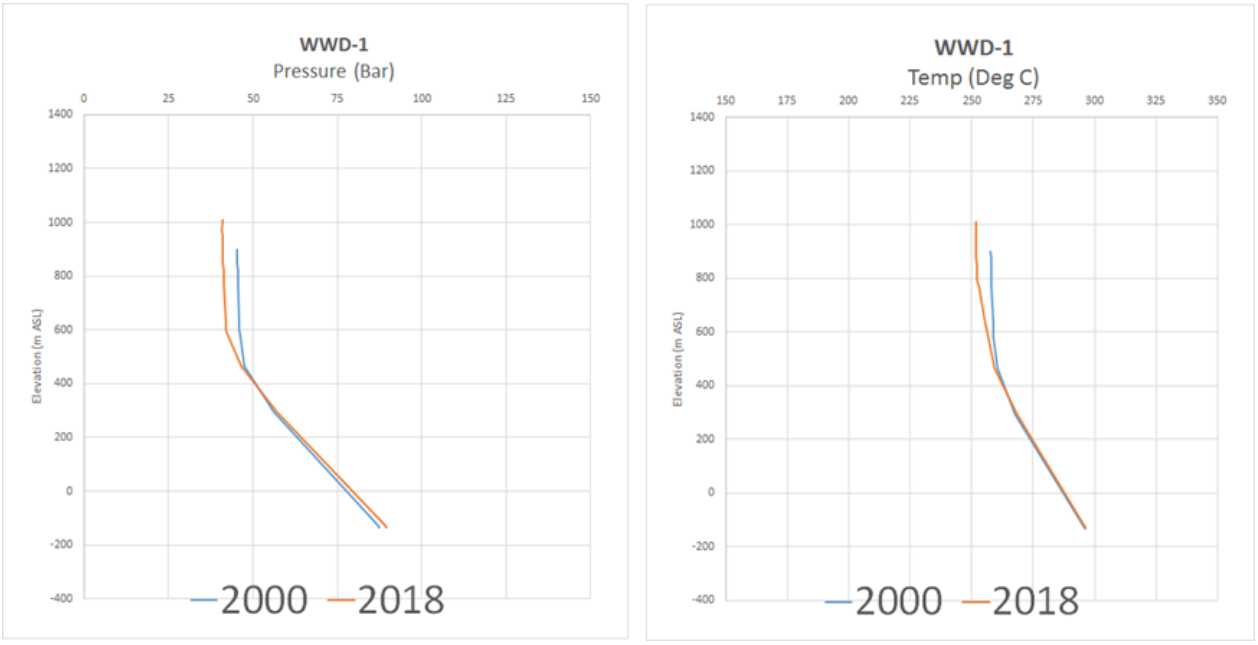

Figure 10: Comparison of reservoir pressure and temperature between pre-exploitation time (year 2000) and year 2018.

Besides pressure-decline trends, the discharge enthalpy trends observed in the wells also provide additional constraints for calibrating the numerical model. Throughout the period of production, the enthalpy of the dry steam wells in the MBA, MBB, MBD and MBE pads remained constant and the model was able to match the enthalpy pattern well.

Initial liquid saturation is one of the major unknowns in the steam cap reservoir part and we relied on the application of superheat data to constrain it. Timing of development, area and degree of superheat as measured in the wellbore were matched by adjusting initial water saturation. Fracture-to-matrix connection parameters were also adjusted to obtain superheat matches. General distribution of the superheat degree in the model has been consistent with field measurements. The highest superheat degree of 20^{o}C occurs in the area around the MBB pad and other areas of the steam cap have a maximum superheat degree of 10^{o}C (Figure 11).

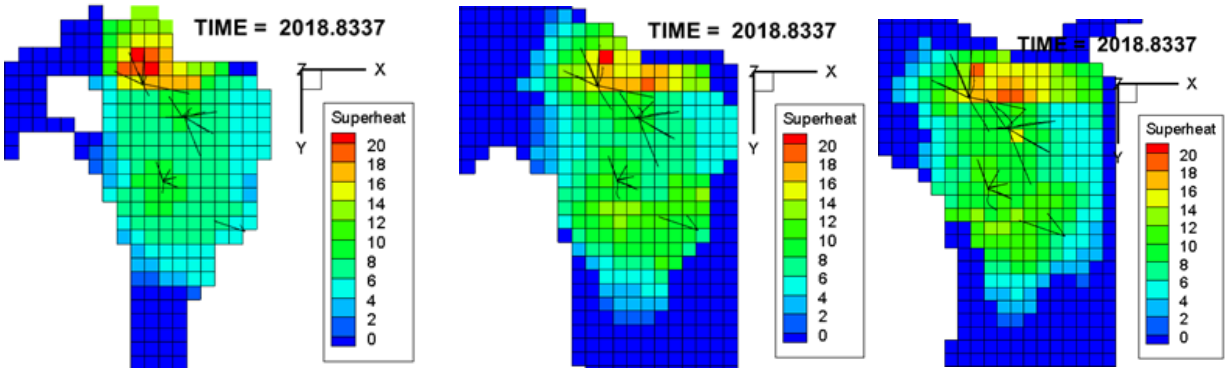

Figure 11: Map view of modeled superheat at K=1 - 3 (1200 to 600 m) at the northern steam cap reservoir.

The results of the history matching show that the newly developed reservoir model successfully simulated the behavior of the reservoir under historical conditions of production and injection. Pressure decline trends determined from the well surveillance have been matched. Enthalpy trends measured from the production wells have been closely simulated by the numerical model. Therefore, the model was adequately calibrated for use in forecasting future reservoir behavior under different production scenarios.

5. RESERVOIR FORECAST

5.1 Forecast Methodology

The quality of pre-exploitation and history matches obtained for the wells give confidence that the newly developed numerical model was a reasonable tool to evaluate alternative Wayang Windu development strategies. The in-house Star Energy program called ToughRunner was used. This program runs the reservoir simulator (TOUGH2) and the wellbore simulator (Geoflow) in forecast mode. Initially, the program reads pressure for the feedzones from the TOUGH input file and then calculates enthalpy using temperature or saturation data also from the input file. This is just an approximation for flowing enthalpy. The reservoir pressures and enthalpies are then used to calculate the peak well deliverability using Geoflow with the Duns correlation. The program calculates the peak capacity of all production wells, whether open or closed, and adds up the peak capacities of open wells to obtain the peak production capacity of the field. It then compares this peak capacity with the steam requirement for the field. If the peak capacity is more than the requirement, all wells will be throttled proportionally to match the steam requirement. Otherwise, make-up wells will be opened until the steam requirement is satisfied. Make-up wells will only be activated when their deliverability is greater than or equal to some specified economic limit, which is currently set at 6 kg/s of steam production. When no more make up wells are available or all available make up wells are not economic to drill then the turbine will operate at a lower pressure reducing the steam demand. This is defined as the turbine operating in “floating” mode and marked as “end of production plateau period”. At this point, the turbine inlet pressure will be reduced. For the current reservoir forecast, a 2 psi pressure-drop was applied. A drop in turbine inlet pressure produces a drop in separator pressure in all separators attached to that turbine. This produces a drop in the wellhead pressure for the connected wells. The pressure drop between the separator and turbine and also between separators and wells is updated using the formula

$$\Delta p_{new} = \Delta p_{old} \left(\frac{W_{new}}{W_{old}} \right)^2 \frac{p_{old}}{p_{new}} \tag{8}$$

Therefore, output from the reservoir forecast include: 1) a forecasted steam production profile (or can be converted into a forecasted power generation profile) and 2) the predicted number of make-up wells needed to sustain steam extraction during the production plateau period.

One key information required to conduct reservoir forecasting using ToughRunner is the value of the PI (productivity index) at each feedzone of the wells. For the existing wells, the PI of each permeable zone was calibrated with the historical evolution of pressure and enthalpy (2). For the future make-up wells, the PI was calibrated using the current average production of the existing wells. In forecasting reservoir performance with the current model, all new wells were assumed to operate at a constant wellhead pressure of 13 bar and separation pressure of 11.5 bar.

5.2 Forecast Results

Using the calibrated numerical model, reservoir performance forecasts were run for three (3) different production scenarios:

1. Scenario 1: Continue 227 generation and future make-up wells were only steam wells drilled to the maximum depth of +400 m SL. It was assumed that the make-up wells were situated mostly in the northern part of the field. The model suggested that the 227 MW of production plateau could only be sustained until the year 2031. The forecasted decline rate of 4.9% from the model was consistent with the observed natural decline rate of 5% (Figure 12). Natural decline rate is defined as the decline rate that excludes production decline due to flow assurance issues in the wellbore such as scaling. It is typically calculated by plotting the well production rate right after the well clean-out programs. Numerical modeling with TOUGH2 is not capable of simulating the chemical reactions that result in scale development in the wellbore and, therefore, the actual decline rate taken for quality checking of the forecasting simulation is the decline rate where the impact of wellbore scaling is neglected.

2. Scenario 2: Continued 227 MW generation and future make-up wells included brine wells drilled to a maximum depth of -400 m SL. The ratio between the number of steam and brine wells on future make-up wells is set at 2:1. It was assumed that the make-up wells were widely distributed across the field. With this development scenario, the model suggests that the production plateau of 227 MW could be sustained until the end of the contract period or longer. A more balanced extraction between the steam cap and brine reservoir sections in Development Scenario 2 promoted steam cap growth as indicated by increased enthalpy. In addition, Scenario 2 has less production interference than Scenario 1 due to greater well separation. As a result of steam cap expansion and less production interference, Development Scenario 2 outperforms Scenario 1 in terms of the length of the production plateau period and a less aggressive drilling program requirement.

3. Scenario 3: Increase generation to 287 MW in 2023 and the distribution of candidate wells for future drilling program was similar to the one used in Scenario 2. The results from the model suggested that the Wayang Windu reservoir was capable of supporting 287 MW generation (the existing 227 MW plus the proposed additional 60 MW generation), provided that the fracture permeability with a magnitude of > 60 millidarcy can be found in deep reservoir section (0 to -400 m ASL elevation)

as currently assigned to the reservoir model. Brine production in Scenario 3 was higher than that of Scenario 2 which led to a higher steam cap expansion rate as indicated by earlier changes of produced enthalpy from liquid into dry steam.

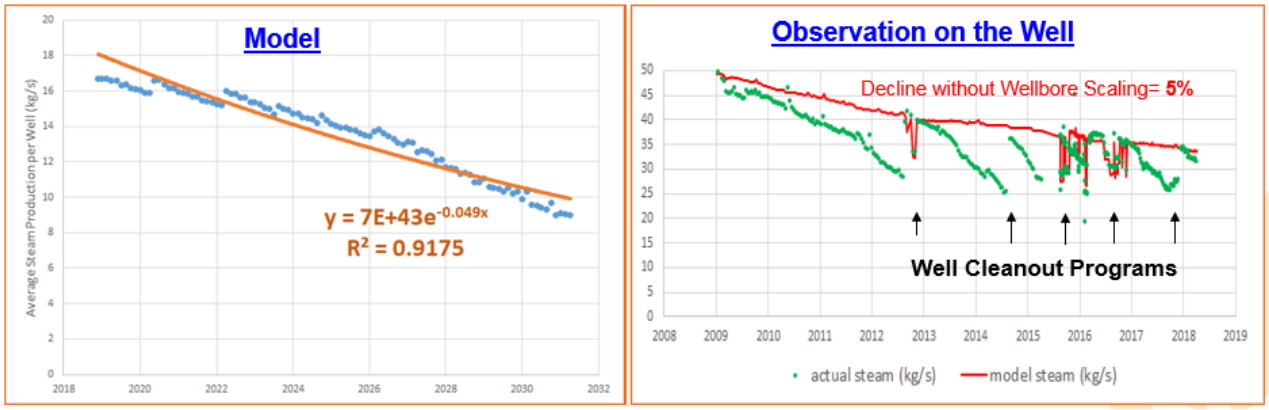

Figure 12: Forecasted and observed production decline rates from the model simulations and observed values.

6. SUMMARY

A numerical model of the Wayang Windu reservoir was recently developed using the TOUGH2 simulator and was calibrated to measured initial state conditions and historical production over 18 years with reasonable results. The first key takeaway from the modelling exercise is a confirmation of a northern reservoir boundary which excludes the potential NW reservoir extension that was previously indicated by resistivity anomaly distributions from MT data. Spending cost for drilling the delineation well to the NW area can therefore be prevented. Modelling also helps the asset team to understand the cause of the recently observed inclining water level in the wellbore is the inclining water level in the reservoir due to imbalanced fluid extraction between the steam cap and liquid reservoir sections. Increasing production from the liquid reservoir section is key to future reservoir management in Wayang Windu. Future make-up wells in the brine reservoir is critical to support both; 1) continuance of 227 MW generation until the end of the contract period and 2) supporting organic growth. Therefore, it is prudent to establish drilling capabilities given the generally lower success rate in drilling into the deep reservoir to date. In addition, risks related to sustainability of future deep brine wells to produce from the deep liquid feedzones should also be addressed. Calcite scaling has formed in several deep wells which reduces or prevents flow from deep brine feedzones in the wellbore.

REFERENCES

Masri, A. and Barton C.: Structural Permeability Assessment Using Geological Structural Model Integrated with 3D Geomechanical Study and Discrete Facture Network Model in Wayang Windu Geothermal Field, West Java, Indonesia. Proceedings, 40th Workshop on Geothermal Reservoir Engineering, Stanford University, Stanford, CA (2015).

Parini, M. and Jarach, F.: Evaluation of geothermal resources with mathematical modeling combined with a probabilistic approach. Proceedings, 8th International Conference on Alternative Energy Sources, Miami (1987).

O'Sullivan, M.J., Pruess, K., and Lippmann, M.J.: Geothermal Reservoir Simulation: The State-of-practice and Emerging Trends. Proceedings, World Geothermal Congress, Kyushu, Japan (2000).

Finsterle, S., and Pruess, K.: Application of Inverse Modelling to Geothermal Reservoir Simulation. Proceeding, 22nd Workshop on Geothermal Reservoir Engineering, Stanford University, Stanford, CA (1997).